Rigid rod anchored to infinite membrane

Kunkun Guo, Feng Qiu,[a] Hongdong Zhang, and Yuliang Yang
The Key Laboratory of Molecular Engineering of Polymers, Ministry of Education, Department of Macromolecular Science, Fudan University, Shanghai 200433, China

(Received 31 January 2005; accepted 30 June 2005; published online 23 August 2005)

We investigate the shape deformation of an infinite membrane anchored by a rigid rod. The density profile of the rod is calculated by the self-consistent-field theory and the shape of the membrane is predicted by the Helfrich membrane elasticity theory [W. Helfrich, Z. Naturforsch. **28c**, 693 (1973)]. It is found that the membrane bends away from the rigid rod when the interaction between the rod and the membrane is repulsive or weakly attractive (adsorption). However, the pulled height of the membrane at first increases and then decreases with the increase of the adsorption strength. Compared to a Gaussian chain with the same length, the rigid rod covers much larger area of the membrane, whereas exerts less local entropic pressure on the membrane. An evident gap is found between the membrane and the rigid rod because the membrane's curvature has to be continuous. These behaviors are compared with that of the flexible-polymer-anchored membranes studied by previous Monte Carlo simulations and theoretical analysis. It is straightforward to extend this method to more complicated and real biological systems, such as infinite membrane/multiple chains, protein inclusion, or systems with phase separation. © *2005 American Institute of Physics*.
[DOI: 10.1063/1.2008248]

I. INTRODUCTION

Biological and biomimetic membranes, such as the plasma membrane of cells, consist of a lipid bilayer, membrane proteins, glycolipids, and various types of macromolecules.[1] The proteins can be classified into two types: transmembrane proteins and peripheral proteins. Transmembrane proteins are rigid inclusions in the membranes. Peripheral proteins, such as caveolin, are less invasive biologically, and they can be separated from the membrane more easily than transmembrane proteins. Many of these protein/membrane compounds carry out important biological tasks such as signal transduction, pore or ion channel formation, and cytoskeleton binding, probably involving in endocytosis and exocytosis processes.[2–4]

The interactions of peripheral proteins with lipid membranes that lead to protein binding are extraordinary complex and not completely understood yet.[5] A prominent role is played by hydrophobic forces, which are significantly influenced by the chain stiffness, topological architectures typical of these proteins. To model the effect of proteins on the membrane, polymer/membrane compounds have been carefully investigated.[6,7] When polymers are anchored or brought to a membrane on one side, the conformational fluctuations of the polymers are reduced due to the restriction of available space, subsequently inducing membrane shape deformation.[6]

A number of theoretical studies have devoted to analyze the effect of polymer chains anchored on fluid membranes. The inhomogeneity of the local bending rigidity and spontaneous curvature of a homogeneous membrane would be induced by the chain segments floating on the membrane.[6–9] Furthermore, the configurational entropy of the polymer would be decreased due to the confined space, which in turn exerts an inhomogeneous pressure patch on the membrane, giving rise to a conelike shape close to the anchor.[10–12] It has been found that with nonzero anchoring distance the membrane has the possibility of bending away from the polymer in the case of weak adsorption, while it would bend towards the polymer on condition of sufficiently strong adsorption.[10,13] In contrast, as the adsorption strength increases, the membrane would not change the sign of curvature without anchoring distance.[10]

Up to now, most of the studies have assumed that the grafted polymer chains are flexible and the influence of the rigidity of the chains is seldom considered.[13] In this paper we will use a combined self-consistent-field theory (SCFT) and Helfrich membrane elasticity theory to investigate the rigid-rod-anchored infinite, flat membrane system. We have applied a similar method, i.e., combining the membrane curvature theory for closed vesicles and SCFT for polymers, to predict the shape changes of the flexible polymer-chain-anchored vesicles.[14] Because the rod is rigid and the membrane is curved, a finite gap exists between the membrane and the rigid rod. Furthermore, the end-to-end distance of a rigid rod is much larger than that of a flexible polymer with the same chain length, thereby it is naturally expected that the membrane will exhibit different bending behaviors. The tension and bending rigidity of the membrane also play important roles in the deformation behavior.

The paper is organized as follows. In Sec. II, a detailed description of our method, which combines SCFT of the rod and curvature elasticity theory of the membrane, is presented. In Sec. III we present the results and discuss the influences of the adsorption of the rigid rod to the membrane, the rod length, as well as the surface tension and bending

[a]Author to whom correspondence should be addressed. Electronic mail: fengqiu@fudan.edu.cn

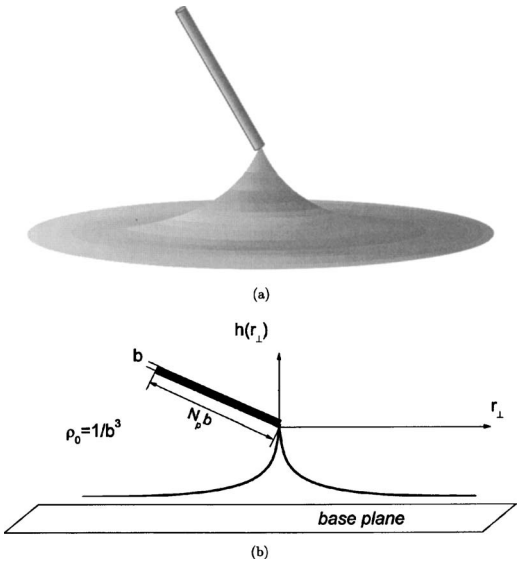

FIG. 1. Schematic illustration of one end of a rigid rod with length $N_p b$ anchored on an infinite membrane: (a) three-dimensional (3D) illustration and (b) coordinate system. The membrane height at $\mathbf{r}_\perp$ is $h(\mathbf{r}_\perp)$, with $\mathbf{r}_\perp$ the coordinate in the base plane. In a system with axis symmetry, $\mathbf{r}_\perp$ reduces to the distance to the origin r.

rigidity of the membrane. The results are compared with that of a polymer-anchored membrane whereas possible. Finally a brief conclusion is given in Sec. IV.

II. MODEL

We consider a rod/membrane system in which the rod is rigid and consists of N_p segments. One end of the rigid rod is anchored to the infinite, flat membrane in a solution with n_s solvent molecules, as illustrated in Fig. 1. The diameter of the rod is taken to be the unit length b. For simplicity, we define the segment size of the rod b equal to the size of the solvent. Note that the statistical segment size plays the same role as the Kuhn length of a Gaussian chain. The membrane usually makes up of amphiphilic short chains and the lateral unit length of the membrane is also reasonably assumed to be b. With these assumptions the density ρ_0 of the rod, membrane, and solvents are equal, i.e., $\rho_0=1/b^3$. We also assume that the membrane is impenetrable to the rigid rod but penetrable to the solvent molecules. Thus no interaction between the solvent and the membrane is introduced in the present model.

We now define the microscopic order parameters of the solvents and the rod. The dimensionless solvent density operator is defined as $\hat{\rho}_s(\mathbf{r})=(1/\rho_0)\Sigma_{i=1}^{n_s}\delta[\mathbf{r}-\mathbf{R}_s^i]$, and the dimensionless rod density operator as $\hat{\rho}_p(\mathbf{r})=(1/\rho_0)\int_0^{N_p}d\tau\delta(\mathbf{r}-\mathbf{R}_p(\tau))=(1/\rho_0)\int d\hat{\mathbf{n}}\int_0^{N_p}d\tau\delta(\mathbf{r}-\mathbf{R}_m(0,0)-\tau\hat{\mathbf{n}})$. $\mathbf{R}_s^i$ and $\mathbf{R}_p(\tau)$ represent the spatial position of the solvent i and the segment τ of the rigid rod, respectively. $\mathbf{R}_m(u,v)$ denotes the position of the membrane, and u,v are curvilinear coordinates in the membrane surface. The unit vector $\hat{\mathbf{n}}=\hat{\mathbf{n}}(\phi,\theta)$, where azimuth $\phi\in[0,2\pi)$ and zenith $\theta\in[0,\pi)$, denotes that the rod can freely gyrate around $\mathbf{R}_m(0,0)$ (it however cannot penetrate the membrane), where $\mathbf{R}_m(0,0)$ is the anchoring position of the rigid rod, as shown in Fig. 1(b).

The interaction potentials can be written as $\beta\hat{V}_{\mathrm{ps}}=(\chi/\rho_0)\Sigma_{i=1}^{n_s}\int_0^{N_p}d\tau\delta(\mathbf{R}_p(\tau)-\mathbf{R}_s^i)=\chi\rho_0\int d\mathbf{r}\hat{\rho}_p(\mathbf{r})\hat{\rho}_s(\mathbf{r})$ for polymer/solvent and $\beta\hat{V}_{\mathrm{pm}}=\eta b\int dA\int_0^{N_p}d\tau\delta(\mathbf{R}_p(\tau)-\mathbf{R}_m(u,v))=\eta\rho_0 b\int dA\hat{\rho}_p(\mathbf{R}_m(u,v))$ for polymer/membrane, where $\beta=1/k_BT$ and χ and η are the interaction parameters of polymer/solvent and polymer/membrane, respectively. dA is the surface element.

The thickness fluctuations can be ignored provided that the thickness $d(\simeq b)$ of the membrane bilayer is small compared to other relevant length scales of the problem (i.e., $d\ll N_p b$ length of the rigid rod). Then the thermodynamic property of the fluid membrane can be coarse-grained and well described by the Helfrich Hamiltonian. The conformation of the membrane can be simply described by the Monge gauge, in which $\mathbf{R}_m=[\mathbf{r}_\perp,h(\mathbf{r}_\perp)]$, where the surface height $h(\mathbf{r}_\perp)$ is defined with respect to the base plane $h(\mathbf{r}_\perp)=\mathrm{const}$ and $\mathbf{r}_\perp$ is the coordinate in the base plane, as shown in Fig. 1(b). Assuming a nearly flat membrane of fixed topology (in which the Gaussian curvature can be ignored), the Hamiltonian of the membrane is written as[15]

$$\beta H_m^0[\mathbf{R}_m(u,v)]=\frac{1}{2}\int d\mathbf{r}_\perp[\lambda(\nabla_\perp h(\mathbf{r}_\perp))^2+\kappa(\nabla_\perp^2 h(\mathbf{r}_\perp))^2], \tag{1}$$

where κ is the bending rigidity of the fluid membrane (in units of k_BT) and λ is the surface tension. The Laplacian $\nabla_\perp^2 h$ equals to the sum of the principal curvatures of the infinite membrane, while $\frac{1}{2}(\nabla_\perp h(\mathbf{r}_\perp))^2$ gives the increase of membrane area per unit projected area due to the membrane tilt $\nabla_\perp h(\mathbf{r}_\perp)$. Since Eq. (1) is only valid for linear perturbations of the planar membrane, to avoid attacking the nonlinear region in the numerical calculation, the parameters used in what follows ensure that the maximum values of either $|\nabla_\perp h(\mathbf{r}_\perp)|$ or $|\nabla_\perp^2 h|$ are on the order of 0.01. The bending rigidity κ of the membrane is assumed independent of the rod anchoring. Early studies by Hiergeist and Lipowsky on polymer-decorated membranes pointed out that a polymer can modify κ.[16] By using a small curvature expansion, the authors derived the effective value of κ, showing that the correction was much smaller than the bare value of κ in the absence of polymers. In the present model, as will be shown later, an extra (entropic) pressure term due to the spatial confinement of the anchored rod by the impenetrable membrane is obtained in the equation that determines the shape of the membrane. Therefore, an effective bending rigidity κ_{eff} is obtained by combining the bare value κ with the entropic pressure.

The present rigid-rod model is a crude approximation for a stiff polymer, in which the bending energy is given by[17,18]

$$H_p^0[\mathbf{R}_p(\tau)]=\frac{l_0}{2}\int_0^{N_p}d\tau\left[\frac{d^2\mathbf{R}_p(\tau)}{d\tau^2}\right]^2, \tag{2}$$

where $d^2\mathbf{R}_p(\tau)/d\tau^2$ is the local curvature of the chain and l_0 is the persistence length measuring the correlations between tangent vectors at different sites of the chain. The rigid-rod model is recovered as a special case for $l_0\to\infty$ and $d^2\mathbf{R}_p(\tau)/d\tau^2\to 0$. Therefore, it is reasonable to assume

$H_p^0[\mathbf{R}_p(\tau)]$=const in the present model, which leads to a great simplification of numerical calculations.

Then the partition function of such system can be written in the following form:

$$\Xi = \mathcal{N}\frac{1}{n_s!}\int \prod_{i=1}^{i=n_s} \mathcal{D}\mathbf{R}_s^i \int \mathcal{D}\mathbf{R}_p \times \exp\{-\beta H_p^0[\mathbf{R}_p(\tau)]\} \int \mathcal{D}\mathbf{R}_m(u,v) \times \exp\{-\beta H_m^0[\mathbf{R}_m(u,v)]\}\exp\{-\beta \hat{V}_{\mathrm{ps}} - \beta \hat{V}_{\mathrm{pm}}\}\delta(1-\hat{\rho}_s - \hat{\rho}_p)\delta(\mathbf{R}_m(0,0)-\mathbf{R}_p(0))\delta\left[\rho_0 \int_{\mathbf{r}\in\mathbf{R}_m^{\downarrow}(u,v)} d\mathbf{r}\hat{\rho}_p\right], \quad (3)$$

where $\mathcal{N}$ is a constant, $\beta=1/k_BT$, and $\mathbf{r}\in\mathbf{R}_m^{\downarrow}(u,v)$ or $\mathbf{r}\in\mathbf{R}_m^{\uparrow}(u,v)$ represents that the position $\mathbf{r}$ is below or above the infinite membrane. $\int\mathcal{D}\mathbf{R}$ denotes a set of path integrals over all possible conformations. Furthermore, three Dirac δ functions are introduced: the first one realizes the incompressibility condition, the second one means that the end of the rod is anchored to $\mathbf{R}_m(0,0)$, and the third one assures that the rod is always above the membrane.

Following the standard procedure of SCFT,[19] a functional integral $1=\int\mathcal{D}\rho_p\delta(\rho_p-\hat{\rho}_p)$ is inserted into Eq. (3), which permits the representation of the operator $\hat{\rho}_p$ by the function ρ_p. The same is done for $\hat{\rho}_s$, and then the δ functionals are replaced by the standard integral representation. This transforms the partition function into

$$\Xi = \int \mathcal{D}\mathbf{R}_m \int \mathcal{D}\rho_p \int \mathcal{D}\omega_p \int \mathcal{D}\rho_s \int \mathcal{D}\omega_s \times \int \mathcal{D}\pi \int \mathcal{D}\zeta \exp\{-\beta\mathcal{F}\}, \quad (4)$$

where the functional $\mathcal{F}$ is

$$\begin{aligned}\rho_0^{-1}\beta\mathcal{F} = &-\rho_0^{-1}\ln[Q_p\{\omega_p\}\rho_0] - n_s\rho_0^{-1}\ln[Q_s\{\omega_s\}\rho_0] \\ &- \int d\mathbf{r}\omega_p\rho_p - \int d\mathbf{r}\omega_s\rho_s - \int d\mathbf{r}\pi(1-\rho_p-\rho_s) \\ &+ \zeta\int_{\mathbf{r}\in\mathbf{R}_m^{\downarrow}} d\mathbf{r}\rho_p + \eta\int_{\mathbf{r}=\mathbf{R}m} d\mathbf{r}\rho_p + \chi\int d\mathbf{r}\rho_p\rho_s \\ &+ \frac{1}{2}\rho_0^{-1}\int d\mathbf{r}_\perp[\lambda(\nabla_\perp h(\mathbf{r}_\perp))^2 + \kappa(\nabla_\perp^2 h(\mathbf{r}_\perp))^2],\end{aligned} \quad (5)$$

where ω_p and ω_s are conjugate potentials of the density field ρ_p and ρ_s, respectively. A field π is introduced to enforce the incompressible constraint and ζ ensures that the membrane is impenetrable to the rigid rod. $Q_p\{\omega_p\}$ denotes the partition function of the rigid rod in the potential field ω_p with one end anchored at point $\mathbf{R}_m(0,0)$ and $Q_s\{\omega_s\}$ is the partition function of solvent molecules in the potential field ω_s. The two partition functions take the following forms, respectively:

$$Q_s\{\omega_s\} = \int d\mathbf{r}\exp\{-\omega_s(\mathbf{r})\}, \quad (6)$$

$$Q_p\{\omega_p\} = \int \mathcal{D}\mathbf{R}_p \exp\left\{-\int_0^{N_p} d\tau\omega(\mathbf{R}_p(\tau))\right\} \times \delta(\mathbf{R}_p(0)-\mathbf{R}_m(0,0)). \quad (7)$$

The partition function Q_p for the rigid rod could be calculated by summing up the exponential of the self-consistent potential ω from the first segment to the last with all possible orientations $\hat{\mathbf{n}}$.

Based on the mean-field approximation, minimizing the functional in Eq. (5) with respect to ζ, ρ_p, ω_p, ρ_s, ω_s, and π, one obtains the following self-consistent equations for the rod and solvents:

$$\omega_p(\mathbf{r}) = \begin{cases}\eta + \chi\rho_s(\mathbf{r}) + \pi(\mathbf{r}), & \mathbf{r}=\mathbf{R}_m, \\ \zeta + \chi\rho_s(\mathbf{r}) + \pi(\mathbf{r}), & \mathbf{r}\in\mathbf{R}_m^{\downarrow}, \\ \chi\rho_s(\mathbf{r}) + \pi(\mathbf{r}), & \mathbf{r}\in\mathbf{R}_m^{\uparrow},\end{cases} \quad (8)$$

$$\omega_s(\mathbf{r}) = \chi\rho_p(\mathbf{r}) + \pi(\mathbf{r}), \quad (9)$$

$$\rho_p(\mathbf{r}) = \frac{1}{\rho_0 Q_p}\exp\left\{-\int_0^{N_p} d\tau\omega_p(\mathbf{R}_p(\tau))\right\}\delta(\mathbf{r}-\mathbf{R}_p(\tau)), \quad (10)$$

$$\rho_s(\mathbf{r}) = \frac{n_s}{\rho_0 Q_s}\exp\{-\omega_s(\mathbf{r})\}, \quad (11)$$

$$1 = \rho_p(\mathbf{r}) + \rho_s(\mathbf{r}), \quad (12)$$

$$0 = \rho_0\int_{\mathbf{r}\in\mathbf{R}_m^{\downarrow}} d\mathbf{r}\rho_p(\mathbf{r}). \quad (13)$$

Further performing the variation of the functional $\mathcal{F}$ with respect to the shape of the membrane,[14] one arrives at the equilibrium shape equation for the infinite membrane,

$$[\zeta\rho_p(\mathbf{R}_m) + \eta b\mathbf{n}\cdot\nabla\rho_p(\mathbf{R}_m)] - [\eta b\rho_p(\mathbf{R}_m) + \lambda\rho_0^{-1}]\nabla_\perp^2 h + \kappa\rho_0^{-1}\nabla_\perp^4 h = 0, \quad (14)$$

where $\mathbf{n}\cdot\nabla\rho_p(\mathbf{R}_m)$ denotes the concentration gradient of the rigid rod along the normal direction on the membrane. The first-order derivative $(\nabla_\perp h)$ is set to be zero on the boundary and the anchored position keeps constant to achieve the shape of the infinite membrane. The extra pressure $(\zeta\rho_p(\mathbf{R}_m))$ originates from the reduction of the rod configuration entropy due to the spatial confinement by the impenetrable membrane. The extra tensile stress $(\eta b\rho_p(\mathbf{R}_m))$ comes from the adsorption of the rod segments onto the membrane. Moreover, the adsorption of the rod onto the membrane also results in additional pressure $\eta b\mathbf{n}\cdot\nabla\rho_p(\mathbf{R}_m)$, which also reflects the membrane and tends to contact more rod segments if the interaction is favorable, i.e., $\eta<0$.

The rotation of the rod is much faster than the deformation of the membrane, since the rotational correlation time for small membrane proteins is usually around 10^{-8} s while the typical time scale of the shape fluctuations for vesicles at 100-nm scale is about 10^{-4} s.[20,21] Therefore, the free end of the rod only touches the membrane transiently and the touching point will be randomly distributed around the grafting

point in Fig. 1. After ensemble averaging, effectively the system can be assumed to be axis symmetric, which greatly simplifies the calculation. We solve all the self-consistent equations and the shape Eq. (14) in the axis-symmetric coordinate system, in which $\mathbf{r}_\perp$ reduces to a scalar r, as shown in Fig. 1. The box size used to calculate the rod density is $L_r=12$ and $L_h=24$ with $\Delta h=0.1$ and $\Delta r=0.1$. We set $\Delta\tau=0.1$ and $b=0.1$ and also fix $\zeta=3$. [We found that this value of ζ is high enough to ensure no rod segments appearing below the (impenetrable) membrane.] In order to solve the self-consistent equations [Eqs. (8)–(14)], we first assume that the initial shape of the membrane is flat. We solve the self-consistent equations with no slope boundary and obtain ρ_p by using the real-space algorithm of Drolet and Fredrickson.[22] Then the solved ρ_p can be inserted into the shape equation [Eq. (14)] to obtain the new membrane shape, in which the fourth-order differential equation is solved by Gaussian elimination with partial pivoting,[23] as well as with the boundary condition of $(\partial/\partial r)h(r=\infty)=0$ and $h(0)=0$. We again solve the self-consistent equations [Eqs. (8)–(14)] to obtain the ρ_p with this new shape of the infinite membrane as well as the changed potentials ω. This procedure is iterated until the convergence condition has been reached, in which the difference of the boundary height satisfies $\Delta h(r=\infty)=10^{-4}$ between two successive iterations. With this condition, the equilibrium shape of the membrane and the configuration of the rigid rod are finally obtained. To avoid the finite edge effect, the lateral size of the infinite membrane is chosen more than $50N_pb$.

III. RESULTS AND DISCUSSION

Figure 2 depicts the shape of the rod-anchored membrane with $\eta=0$, i.e., no adsorption between the membrane and the rigid rod. Close to the anchoring, the membrane shows conelike shape and bends away from the rod. Since the length of the rigid rod, $R_p=N_pb$, is much larger than the coil size of a Gaussian chain with the same chain length ($R_p=b\sqrt{N_p}$), the "corona" of the rod formed above the membrane is much larger than that of the corresponding Gaussian chain. Therefore more free space for the rigid rod is available, which would provide more opportunity of the rod to exert entropic pressure on the membrane. Polymer chains, however, exert largely an inhomogeneous pressure on the neighborhood and on the anchoring position, resulting from highly local conformation fluctuations of the polymers according to a previous scaling theory.[7] Of course, other distinguished differences also exist between the anchoring of the Gaussian chain and rigid rod. In fact, in the case of rigid rod anchoring, not all rod segments could exert entropic pressure on the membrane, and a gap exists between the membrane and the rigid rod at the equilibrium state because of the rigidity of the rod and the continuity of the membrane curvature, as shown in Fig. 2(a). However, the behaviors of the membrane bending away from the anchored Gaussian chain or rigid rod are in agreement with the results of previous Monte Carlo simulations and analytical calculations.[10]

The density of the rod, represented by the gray color, is gradually attenuated from the anchoring position. The densities of the rod along the vertical ($r=0$) and horizontal ($h=0$) directions with $\eta=0$ are shown in Fig. 2(b). Since the rod is freely rotating about the anchoring above the membrane, the density profiles along these two directions are almost identical and thus only one profile is seen. In both cases, the densities drop suddenly from the anchoring position and then decay smoothly further away. Plotting in the logarithmic scale, as shown in the inset of Fig. 2(b), these densities are seen to decay gradually with an exponent of −2, which can be explained as follows: Since the rigid rod rotates freely, its density distribution obeys a simple scaling $\rho_p(r,h)\propto b^2/2\pi(r^2+h^2)$, where $r^2+h^2<N_p^2$ and r,h represents the space position in the cylindrical coordinate.

As shown in the left inset of Fig. 2(a), the membrane height decreases algebrically close to the anchoring position, but exponentially decays far away from it. A similar behavior has also been predicted in a polymer-anchored membrane by means of a perturbation calculation.[11,12] Considering that the

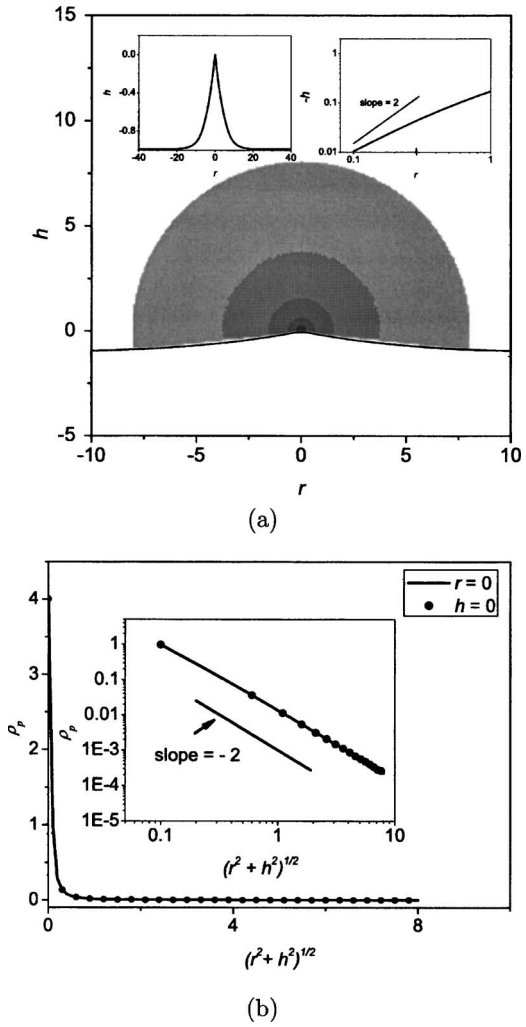

FIG. 2. Shapes of the infinite membrane anchored by a rigid rod with $\eta=0$, $\kappa=0.02$, $N_p=80$, $\lambda=0.001$, and $\chi=0$. (a) The density of the rigid rod is drawn in gray with the logarithmic scale. The shape of the infinite membrane is represented by solid curves. Note the gap between the membrane and the rod. In the left inset, the shape of the whole membrane is drawn; in the right inset, the shape of the membrane nearby the anchoring point is shown in the logarithmic scale. (b) The density profile of the rod along the vertical ($r=0$) and horizontal ($h=0$) directions. In the inset, the same plot is drawn in logarithmic scale.

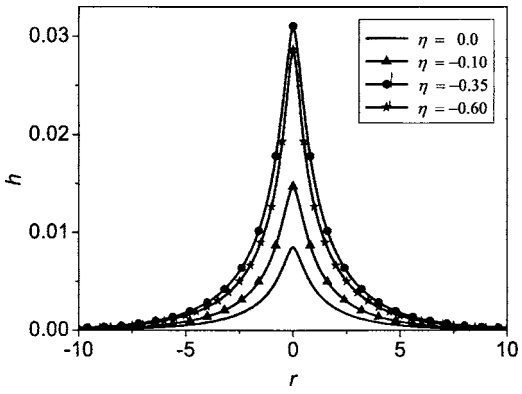

FIG. 3. Shape of the infinite membrane anchored by the rigid rod for different adsorption strengths η with $N_p=40$, $\kappa=1$, $\lambda=0.01$, and $\chi=0$.

entropic pressure, which is in proportion to the density of the rod segments on the membrane, is the main driving force of the membrane deformation and ignoring the contribution of the surface tension (which is safe since the κ term is much greater than the λ term for the parameters in Fig. 2) one can simplify Eq. (14) into

$$\kappa\rho_0^{-1}\nabla_\perp^4 h(\mathbf{r}_\perp) \simeq -\zeta\rho_p(\mathbf{R}_m) \propto -\frac{\zeta b^2}{2\pi r^2}. \tag{15}$$

Near the anchoring the solution of the above equation has an asymptotic form:

$$h(r)\simeq_{r\to\Delta r} -\frac{\zeta}{2\pi b\kappa}\left[\frac{r^2(\ln r)^2}{8} - \frac{r^2\ln r}{4} + \frac{3r^2}{16}\right]. \tag{16}$$

When $r\to\Delta r \ll 1$, keeping only the leading term in the right-hand side of the above equation and taking the logarithm of both sides, we arrive at

$$\log(-h(r)) = c_0 + 2\log r + 2\log|\ln r|, \tag{17}$$

where $c_0=\log\zeta/16\pi b\kappa$. When $r\ll 1$, the last term is negligible when compared to the second term, so $\log(-h(r)) \simeq 2\log r$ follows, which is in agreement with the results plotted in the right inset of Fig. 2(a).

In Fig. 3, the shapes of the rod-anchored membrane are presented for different adsorption parameters η between the membrane and rigid rod. For a clear comparison, all the membranes are vertically moved so that the membrane height at the boundary is zero. As shown in Fig. 3, all the membranes bend away from the rigid rod, and significant deformation only occurs in a range of the order of the rod length. Clearly, with the increase of $|\eta|$ (η goes more negative) the height of the membranes at the anchoring position at first increases and then decreases, as shown in Fig. 3. To be more explicit, the height of the membrane, defined as $\Delta H=h(r=0)-h(r\to\infty)$, is plotted as a function of η in Fig. 4. Simple sketches are drawn in the top of Fig. 4(a) to illustrate the membrane deformation as η changes. Three qualitatively different regions are observed. In region I, where $\eta>0$ (the interaction is repulsive), the pulled height goes up as the interaction changes from repulsion to weak adsorption. In region II, the pulled height increases slowly with the decrease of η, up to certain critical value, it reaches a maximum and then drops down. For high enough adsorption

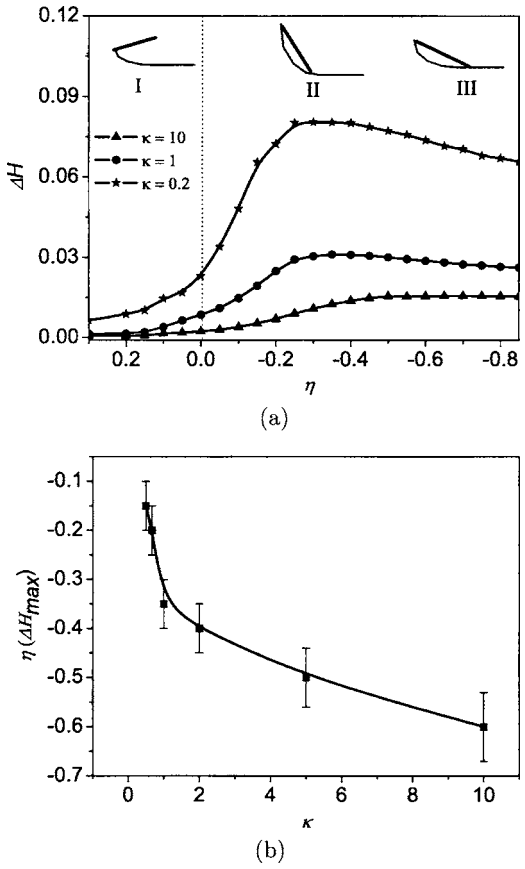

FIG. 4. (a) Plot of the pulled height of the membrane ($\Delta H=h(0)-h(r\to\infty)$) vs adsorption strengths for different bending rigidities $\kappa=0.2$, 1, and 10, other parameters are the same as in Fig. 3. (b) Plot of the value of η at which ΔH attains its maximum vs bending rigidity.

strength, the pulled height will decrease further, and the membrane will become flat again in the last region (III). The competition between the adsorption potential and the membrane curvature energy determines the degree of bending away of the membrane. If the contribution of the bending rigidity is far larger and can suppress that of the interaction potential, the membrane will remain almost flat. Otherwise, the membrane chooses to sacrifice its curvature energy and will be explicitly pulled out. As shown in Figs. 3 and 4(a), the membrane has to bend further away from the rigid rod with the decrease of η in region I. However, further decreasing η results in a decrease of the pulled height in region II. The reason is in the case that the adsorption parameter η becomes strong enough, if all the segments of the rigid rod could cover the membrane, then the adsorption potential is the largest, which is favorable; whereas the bending energy of the membrane is the least in the flat state. Therefore the membrane must become flat again with such strong enough adsorption of the rod, just as the trend shown in Fig. 4. This trend can be deduced by qualitatively analyzing the shape equation [Eq. (14)]. The term $\mathbf{n}\cdot\nabla\rho(\mathbf{R}_m)$ is always positive, with a negative η, it counteracts the inhomogeneous entropic pressure term $\zeta\rho_p(\mathbf{R}_m)$ inflicted by the rigid rod, giving rise to a gradual decrease of the membrane height. For this reason, the pulled height of the membrane does not monotonically increase with the adsorption parameter. The role of the bending rigidity κ is shown in Fig. 4(b), in which the value

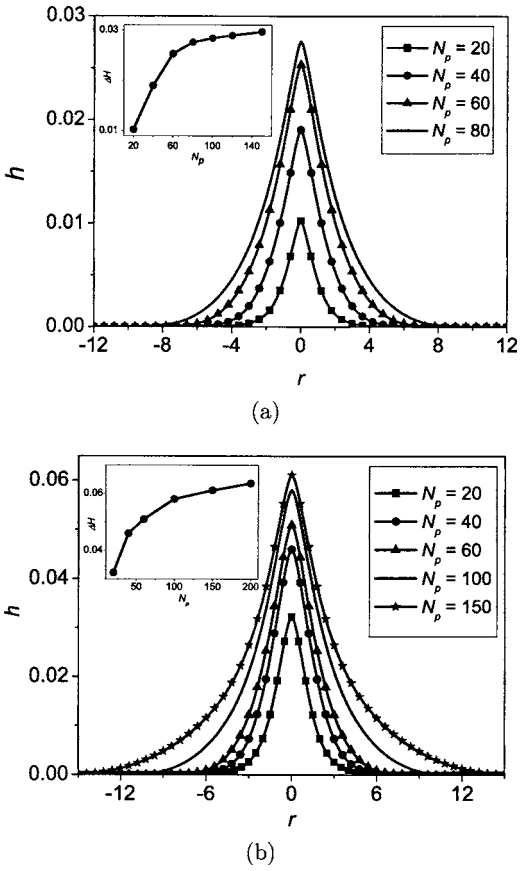

FIG. 5. Shape of the rod-anchored membrane for different rod lengths N_p with $\kappa=1$, $\lambda=0.01$, and $\chi=0$. In the inset the pulled height ΔH is plotted vs the chain length. (a) $\eta=0$ and (b) $\eta=-0.3$.

of η at which ΔH in Fig. 4(a) attains its maximum is plotted. This maximum decreases with the increase of κ and disappears when κ is high enough (in this case when $\kappa>10$). It is interesting to compare this phenomenon to a fixed size membrane adsorbing flexible chains, in which from weak to strong adsorption, as proposed by Kim and Sung, the sign of the membrane curvature will change.[13] The polymer segments can uniformly distribute on the membrane and form a lot of loops without grafting. However, for the rigid rod, the loop conformation is not possible and the influence of the curvature at the boundary has to be taken into account. Thus the infinite membrane will be prone to be flat and not change the sign of the membrane curvature even in the strong adsorption regime.

The shape of the membranes anchored by the rigid rod with different lengths is plotted in Fig. 5. It is seen that all the membranes bend further away from the rigid rod with the increase of the rod length. Note that the coverage on the membrane would monotonically increase with the length of the rigid rod. Therefore longer rods would have more segments to exert inhomogeneous pressure on the membrane, this implies that the membrane would bend further away from longer rods, which is confirmed in Fig. 5 for both $\eta=0$ and $\eta=-0.3$. However, the pulled height is not proportional to the chain length and the pulling effect of the rod becomes much less significant for longer rods. This is quantitatively described in the insets of Figs. 5(a) and 5(b), in

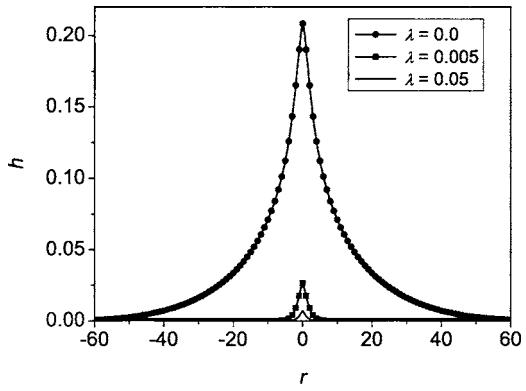

FIG. 6. Shape of the rod-anchored membrane for different surface tensions λ with $N_p=40$, $\kappa=1$, $\eta=0$, and $\chi=0$.

which the (maximum) pulled height of the membrane $h(0)$ against the rod length N_p is plotted. The pulled height approaches a finite limit when $N_p \gg 100$ for both $\eta=0$ and $\eta=-0.3$. The reason is that a finite gap exists between the membrane and rigid rod, especially for a longer rod. Thus not all the segments of the rigid rod can effectively exert entropic pressure that causes bending of the membrane. Moreover, for the same adsorption strength, a similar effect has been observed, irrespective of the flexibility of the anchoring chains.[14] The membrane is already full of chain segments at this specific state and is not able to "eat" segments any more.

Figure 6 illustrates the effect of the membrane surface tension. The membrane bends away from the rigid rod for all positive tensions with $\eta=0$. For the zero surface tension, $\lambda=0$, the pulled height is the highest and decays more slowly from the anchoring position. In contrast, for high λ, the pulled height is much lower and decays much more rapidly away from the anchoring. For a small fluctuation inflicted on the infinite membrane: when $\lambda>0$, the surface tension determines the nature of the long-wavelength fluctuations, $\langle h^2\rangle \propto k_BT/(2\pi\lambda)\ln(L_B)$; when λ is close to zero, the bending rigidity determines the nature of the fluctuations, $\langle h^2\rangle \propto k_BT/(2\pi\kappa)L_B^2$, where L_B is the length of the base plane.[15] Then, the pulled height for $\lambda>0$ will decay more rapidly than that of $\lambda=0$, as well as the pulled height will be higher with smaller surface tension. Kohyama also proposed that the flat membrane can exhibit an undulating shape, which significantly decreases the surface tension.[24]

Recent elegant experiments demonstrated that the control of the surface tension may be achieved via micropipette aspiration, facilitating studies of the effect of tension on membrane elasticity and water permeability.[25,26] With these experiments the surface tension (λ) parameter of the membranes was estimated to be 0.01–0.1 pN/nm, which is about $0.0025k_BT/\text{nm}^2$–$0.025k_BT/\text{nm}^2$, thus the magnitude of the surface tension used in our numerical calculation agrees

fairly with the parameter obtained from the experiments. The anchoring rigid rod exerts not only the inhomogeneous entropic pressure but also the inhomogeneous surface tension on the membrane with interaction potential between the membrane and rigid rod, according to the equilibrium shape equation [Eq. (14)]. Furthermore, the surface tension would be decreased to some extent because of the adsorption interaction (since $\eta<0$) and increased with the repulsion between the rod and membrane. In this case, the membrane is softened with rod adsorption and thereby the pulled height will increase. The effect of the anchoring rigid rod will be involved in larger area of the membrane with lower surface tensions, that is, the inflicted pressure field will be extensively diffused far away from the anchoring position. However, the effective range of the anchoring rod is within the distance of several rod lengths with positive surface tension; the pulled height is not very high and the membrane falls rapidly to flat, as shown in Fig. 6. Therefore, undulations of the membrane induced by positive tension of the membrane itself and extra tension because the external anchoring structures are so small and were ignored in most previous theoretical studies.

Rigid rods such as cytoskeleton anchoring and inclusion increase more or less the bending rigidity of the membrane, which inevitably restrains its thermal fluctuations, as shown by previous experiments.[27,28] For biological membranes primarily composed of a bilayer of phospholipids, the bending rigidity is typically $\kappa=10\sim40k_BT$.[25] The effect of the bending rigidity on the membrane for $\eta=0$ and $\eta=-0.3$ is shown in Fig. 7. The membranes bend further away from the rigid rod as the bending rigidity decreases from $\kappa=10$ to $\kappa=0.5$, which means the membranes with large bending rigidity can resist extra deformation. In the inset of Fig. 7(a) the pulled height is plotted as a function of the bending rigidity of the membrane, in which a distinct linear behavior is observed with a slope of -1, which is exactly what Eq. (16) has expected. We note that, for flexible polymer anchoring, a similar argument predicted the pulled height behaving like $h(r) \propto_{r\to\Delta r} -(k_BT/\kappa)(r/2\pi)$.[11] We therefore also performed a calculation for a flexible chain anchoring and obtained a slope of -0.9, which was slightly different from the rod case (-1). For $\eta\neq0$, the equilibrium shape or the pulled height cannot be described by a single scaling law, it is controlled by the membrane curvature, contact area between the membrane and rod, as well as the configuration entropy loss of the rod. Figure 7(b) shows an example with $\eta=-0.3$, in which $\Delta H=h(0)-h(\infty)$ decreases with the increase of κ, but is slower as compared to the case with $\eta=0$. The reason is that strong adsorption $(\eta<0)$ tends to counteract the bending, which is reflected in Eq. (14) (compare the second and third terms).

The interaction χ between the rod and the solvent is not explicitly included in the Eq. (14). However, the quality of the solvent could potentially affect the shape of the membrane through its interaction with the rod. But this effect is not significant for the rod-grafted membrane since the rod is rigid and the distribution of the rod segment is almost not influenced as long as no phase separation between the rod and the solvent occurs, which needs a high positive χ value

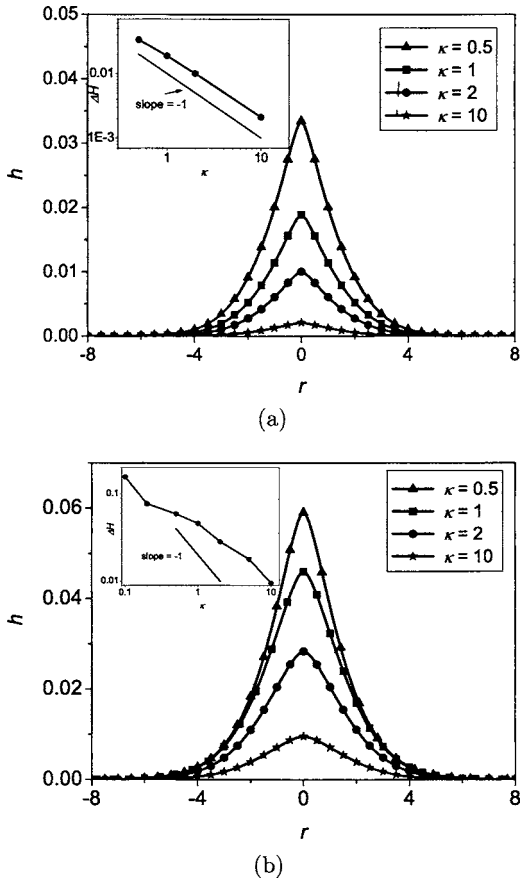

FIG. 7. Shape of the rod-anchored membrane for different bending rigidities κ with $N_p=40$, $\lambda=0.01$, and $\chi=0$. In the inset, the pulled height ΔH as a function of the bending rigidity is drawn in the logarithmic scale. (a) $\eta=0$ and (b) $\eta=-0.3$.

and in reality $\chi<0$ because proteins always have hydrophilic groups interacting with the water solvent. Figure 8 shows the the membrane shape with different χ values for $\kappa=1$ and $N_p=40$. Indeed increasing χ causes a slight decrease of the pulled height ΔH because in a bad solvent the rod prefers to stay close to the membrane, which suppresses the pulling of the membrane, but this effect is not significant as compared to that of other parameters.

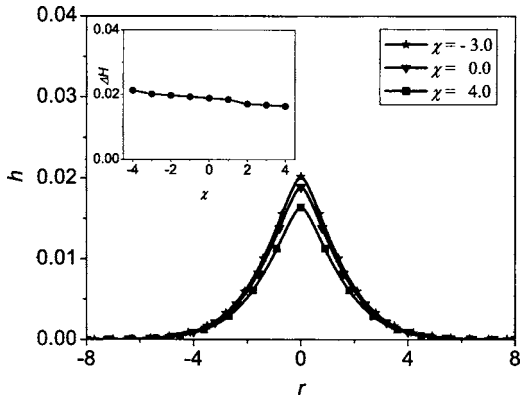

FIG. 8. Shape of the rod-anchored membrane for different χ with $N_p=40$, $\lambda=0.01$, and $\eta=0$. In the inset, the pulled height ΔH as a function of χ is drawn.

IV. CONCLUSION

We have investigated the system of a rigid rod anchored to an infinite membrane by combining the SCFT for the rigid rod and membrane curvature theory. It is found that the membrane bends away from the rigid rod when the interaction between the rod and the membrane is repulsive or weak attractive (adsorption). However, the pulled height of the membrane at first increases and then decreases with the increase of the adsorption strength. An evident gap is found between the membrane and the rigid rod because the membrane's curvature has to be continuous. Compared to a Gaussian chain with the same length, the rigid rod covers much larger area of the membrane, therefore exerts less local entropic pressure on the membrane, which clearly affects the bending extent of the membrane even in zero adsorption strength. Conformations of both the rigid rod and Gaussian chain realize a transition from "mushroom" to "pancake" with the increase of the adsorption strength. Furthermore, the effect of the surface tension and bending rigidity on the membrane deformation are explicitly investigated. The positive tension controls the scope of the membrane that is apparently deformed. However, it does significantly influence the height of the membrane. High bending rigidity of the membrane can resist the pulling effect of the anchoring rod. The physical results presented here can provide valuable insights to various biological processes.

ACKNOWLEDGMENTS

We gratefully acknowledge financial support from the National Natural Science Foundation of China (Grant Nos. 20221402, 20234010, and 20374016). One of the authors (F.Q.) acknowledges the Ministry of Education of China (FANEDD 200225) and the STCSM (Grant No. 02QE14010). We thank Jiafang Wang and Jianfeng Li for useful discussions.

[1] R. Lipowsky and E. Sackmann, in *Structure and Dynamics of Membranes, Handbook of Biological Physics* Vol. 1 (Elsevier, Amsterdam, 1995).
[2] H. G. Doebereiner, E. Evans, M. Krauss, U. Seifert, and M. Wortis, Phys. Rev. E **55**, 4458 (1997).
[3] I. Szleifer, O. V. Gerasimov, and D. H. Thompson, Proc. Natl. Acad. Sci. U.S.A. **95**, 1032 (1998).
[4] V. Frette, , M. A. Guedeau-Boudeville, I. Tsafrir, L. Jullien, D. Kandel, and J. Stavans, Phys. Rev. Lett. **83**, 2465 (1999).
[5] F. Ronzon and B. Desbat, Biochim. Biophys. Acta **1560**, 1 (2002).
[6] R. Golestanian, M. Goulian, and M. Kardar, Phys. Rev. E **54**, 6725 (1996).
[7] P. G. de Gennes, J. Phys. Chem. **94**, 8407 (1990).
[8] J. Brooks, C. Margues, and M. Cates, J. Phys. II **1**, 673 (1991).
[9] R. Podgornik, Europhys. Lett. **21**, 245 (1993).
[10] M. Breidenich, R. R. Netz, and R. Lipowsky, Eur. Phys. J. E **5**, 403 (2001).
[11] T. Bickel, C. Jeppesen, and C. M. Marques, Eur. Phys. J. E **4**, 33 (2001).
[12] R. Lipowsky, Europhys. Lett. **49**, 431 (2000).
[13] Y. W. Kim and W. Sung, Phys. Rev. E **69**, 041910 (2001).
[14] J. F. Wang, K. K. Guo, F. Qiu, H. D. Zhang, and Y. L. Yang, Phys. Rev. E **71**, 041908 (2005).
[15] P. M. Chaikin and T. C. Lubensky, *Principles of Condensed Matter Physics* (Cambridge University Press, Cambridge, 1995).
[16] C. Hiergeist and R. Lipowsky, J. Phys. II **6**, 1465 (1996).
[17] R. R. Netz and D. Andelman, Phys. Rep. **380**, 1 (2003).
[18] J. Kierfeld and R. Lipowsky, Europhys. Lett. **62**, 285(2003).
[19] K. M. Hong and J. Noolandi, Macromolecules **14**, 727(1981).
[20] T. Chou, K. S. Kim, and G. Oster, Biophys. J. **80**, 1075 (2001).
[21] A. G. Zilman and R. Granek, Phys. Rev. Lett. **77**, 4788 (1996).
[22] F. Drolet and G. H. Fredrickson, Phys. Rev. Lett. **83**, 4317 (1999).
[23] A. V. Aho and J. E. Hopcroft, *The Design and Analysis of Computer Algorithms* (Addison-Wesley, Boston, MA, 1974).
[24] T. Kohyama, Phys. Rev. E **57**, 6815 (1998).
[25] R. Bar-Ziv and E. Moses, Phys. Rev. Lett. **73**, 1392 (1994).
[26] E. Evans and W. Rawicz, Phys. Rev. Lett. **79**, 2379 (1997).
[27] A. R. Rvans, M. S. Turner, and P. Sens, Phys. Rev. E **67**, 041907 (2003).
[28] N. Gov, A. G. Zilman, and S. Safran, Phys. Rev. Lett. **90**, 228101 (2003).